Research Paper

T5224, RSPO2 and AZD5363 are novel drugs against functional pituitary adenoma

Sheng Zhong[1,2,*], Bo Wu[2,4,*], Jiahui Li[3], Xinhui Wang[2,5], Shanshan Jiang[3], Fangfei Hu[3], Gaojing Dou[2], Yuan Zhang[2], Chunjia Sheng[2], Gang Zhao[1,2], Yunqian Li[1,2,#], Yong Chen[1,2]

[1]Department of Neurosurgery, The First Hospital of Jilin University, Changchun, China
[2]Clinical College, Jilin University, Changchun, China
[3]Pharmacy College, Jilin University, Chuangchun, China
[4]Department of Orthopaedics, The First Hospital of Jilin University, Changchun, China
[5]Department of Oncology, The First Hospital of Jilin University, Changchun, China
*Equal contribution
[#]Co-corresponding author

Correspondence to: Yong Chen, Yunqian Li; **email:** chenyong_jdyy@126.com, liyunqian_jdyy@126.com
Keywords: bioinformatics, brain science, drug treatment, functional pituitary adenomas, prognosis
Received: April 25, 2019 **Accepted:** October 12, 2019 **Published:** October 26, 2019

ABSTRACT

We tested whether the drugs T5224, RSPO2, and AZD5363 exert therapeutic effects against functioning pituitary adenoma (FPA). We analysed the gene expression profiles of four FPA mRNA microarray datasets (GSE2175, GSE26966, GSE36314, and GSE37153) from the Gene Expression Omnibus database and identified genes differentially expressed in FPA vs control tissues. We then carried out Gene Ontology, Kyoto Encyclopedia of Genes and Genomes (KEGG), and protein-protein interaction network analyses. We also measured the difference in expression of hub genes between human normal pituitary cells and FPA cells using qRT-PCR. Our *in vitro* colony-formation and MTT assays showed that cell viability, number, and the size of clonogenicities were all lower in the presence of T5224, RSPO2, or AZD536 than in controls. Moreover, flow cytometry experiments showed that the incidence of apoptosis was higher in the presence of T5224, RSPO2, or AZD5363 than among controls, and was increased by increasing the doses of the drugs. This suggests these drugs could be used as therapeutic agents to treat FPA. Finally, we found that cFos, WNT5A, NCAM1, JUP, AKT3, and ADCY1 are abnormally expressed in FPA cells compared to controls, which highlights these genes as potential prognostic and/or therapeutic targets.

INTRODUCTION

Functioning Pituitary Adenoma (FPA) accounts for 70% of all pituitary adenomas (PA) [1]. Epidemiological studies have suggested that the incidence and prevalence of pituitary neoplasm might be underestimated at 7.39/100,000/year and 97.76/100,000, respectively [2]. FPA can cause hyper-secretion syndromes, such as hyperprolactinemia, acromegaly, and Cushing disease, or mass effects, such as headaches, hypopituitarism, vomiting, and visual field defects [4]. Based on hormonal activity, FPA is clinically classified mainly as prolactinoma (PRL), growth hormone (GH) tumors, or adrenocorticotropic (ACTH) hormone tumors. Gonadotropin hormone tumors, multiple hormone adenomas, and thyroid-stimulating hormone (TSH) tumors occur only rarely in FPA [3]. The fact that FPA can arise from a wide variety of cancer types makes it complicated to conduct research on FPA's diagnosis, underlying molecular mechanisms, and treatment.

Currently, early diagnosis and treatment have improved, owing to the widespread use of magnetic resonance imaging (MRI) [2]. However, diagnostic methods, such

as measuring hormone levels, MRI, pathological and immunohistochemical assays, etc., are still not accurate nor timely enough to prevent morbidity and consequent mortality due to FPA. Traditional treatments such as Dopamine agonists, surgery, and radiotherapy have limited effectiveness and cause deleterious side effects, including a reduced quality of life in the presence of persistent morbidity and slightly increased mortality [4]. Many types of FPA, especially macroadenomas, have extremely low cure rates [6]. For example, in ~20% of prolactinoma cases, treatment is partially or completely ineffective [5].

Previous studies have demonstrated overexpression of high mobility group A (HMGA) in FPA, possibly due to downregulation of HMGA-targeting microRNAs (miRNAs) [7]. For example, HMGA2 is overexpressed in prolactinoma. In addition, the majority of adenomas show reduced EFEMP1 expression, irrespective of subtype [8]. Other factors like reduced expression of bone morphogenetic proteins (BMP) can cause some adenoma subtypes [9]. In this study, c-Fos, Wnt5A, and Akt3 was identified as hub genes, which could be used to treat FPA. c-Fos is component of AP-1 transcription factors, and T5224 has been reported selectively inhibit AP-1. This drug already be used in phase II human clinical trials in Japan [10]. RSPO2 can block binding of Wnt5A to Fzd7 receptor to antagonize tumor cell migration [49]. AZD5363 is one of Akt3 inhibitors and an apoptosis promoter in prostate cancer [50].

Here, we hypothesized that T5224, RSPO2, and AZD5363 should be effective treatments against FPA. To test this hypothesis, we looked for genes differentially expressed in FPA tissues compared to normal brain controls. We also performed bioinformatics analyses to investigate the molecular processes underlying FPA and used various biochemical and cell biology assays to test the effects of T5224, RSPO2, and AZD5363 treatments.

RESULTS

Identification of differentially expressed genes

We analyzed the gene expression profiles of four FPA mRNA microarray datasets (GSE2175, GSE26966, GSE36314, and GSE37153) from the Gene Expression Omnibus database. There were 19,943 differently expressed genes (DEGs) picked up from GSE2175, of which 12,268 were upregulated while 7675 were downregulated. Altogether, 4635 DEGs were found out from GSE26966, among which 2159 were upregulated and 2476 were downregulated. Among 6472 DEGs were identified from GSE36314 with 2520 upregulated genes and 3952 downregulated genes. Lastly, 2020 DEGs were discovered from GSE37153, in which 2020 genes were upregulated and 1017 were downregulated. There were 178 mutual DEGs among the four datasets (Figure 1A, Supplementary Table 1).

Functional and pathway enrichment analysis

The mutual DEGs were uploaded to DAVID for GO and KEGG pathway analyses (Table 1 and Figure 1C, 1D). The GO analysis results revealed that the mutually upregulated DEGs were mainly associated with several biological processes (BPs), such as mitotic nuclear division, cell division, and chromosome segregation; cellular components (CCs; spindle, microtubule, kinetochore); and molecular functions (MFs; protein binding, ATP binding, microtubule motor activity). For the mutually downregulated DEGs, the GO analyses revealed that they were primarily involved in BPs such as neurotransmitter secretion, neurotransmitter transport, and ion transport; CCs covering cell junctions and plasma membrane; and MFs including calcium ion binding and calcium-dependent protein binding. In addition, KEGG analyses indicated that the mutual DEGs were mainly involved in cell cycle, oocyte meiosis, and p53 signaling pathways, nicotine addiction, GABAergic synapse, and morphine addiction.

Module screening from the PPI network

We also conducted PPI network analyses of the previous 178 mutual DEGs. Genes with degrees ≥ 6 were screened as hub genes based on the STRING database. Altogether, 21 genes were identified as hub genes (Figure 1E–1G), including c-Fos, MYC, BCL2, WNT5A, POMC, NCAM1, JUP, AKT3, ADCY1, FGFR2, GH1, CCND2, TSHB, GHRHR, PPP2R5A, BCR, CAMK2G, ATP2A2, APC, and MAD2L1 (listed in Table 2). MYC had the highest degree of nodes, which was 20. Moreover, after MCODE analysis, 157 nodes and 797 edges were obtained, as well as the top three modules (Figure 2), whose functional annotation and enrichment are shown in Table 3. Enriched function analysis revealed that genes in module 1 were primarily related to cell proliferation, protein complex formation, and negative regulation of apoptosis. In module 2, the genes were mainly enriched in activation of adenylate cyclase activity, adenylate cyclase-activating G-protein coupled receptor signaling pathways, and regulation of lipolysis in adipocytes. Finally, for module 3, the genes were involved in glycoprotein binding, anchored component of membrane, and myelin sheath formation.

Measuring expression of hub genes by qRT-PCR

We performed qRT-PCR in order to conform the expression of cFos, WNT5A, NCAM1, JUP, AKT3, and ADCY1 in normal pituitary cells and FPA cells (GT1-1,

GH3). NCAM1, cFos, AKT3, and ADCY1 were consistently upregulated in FPA cells compared to normal pituitary cells ($P < 0.05$) while WNT5A and JUP were downregulated ($P < 0.05$)., with levels being slightly different across the tested cell lines (showed in Figure 1B).

T5224, RSPO2, and AZD5363 reduce proliferation of FPA cells

We used MTT assay to measure cell survival after T5224, RSPO2, and AZD5363 treatment. As is shown in Figures 3 and 4, with increasing drug concentrations,

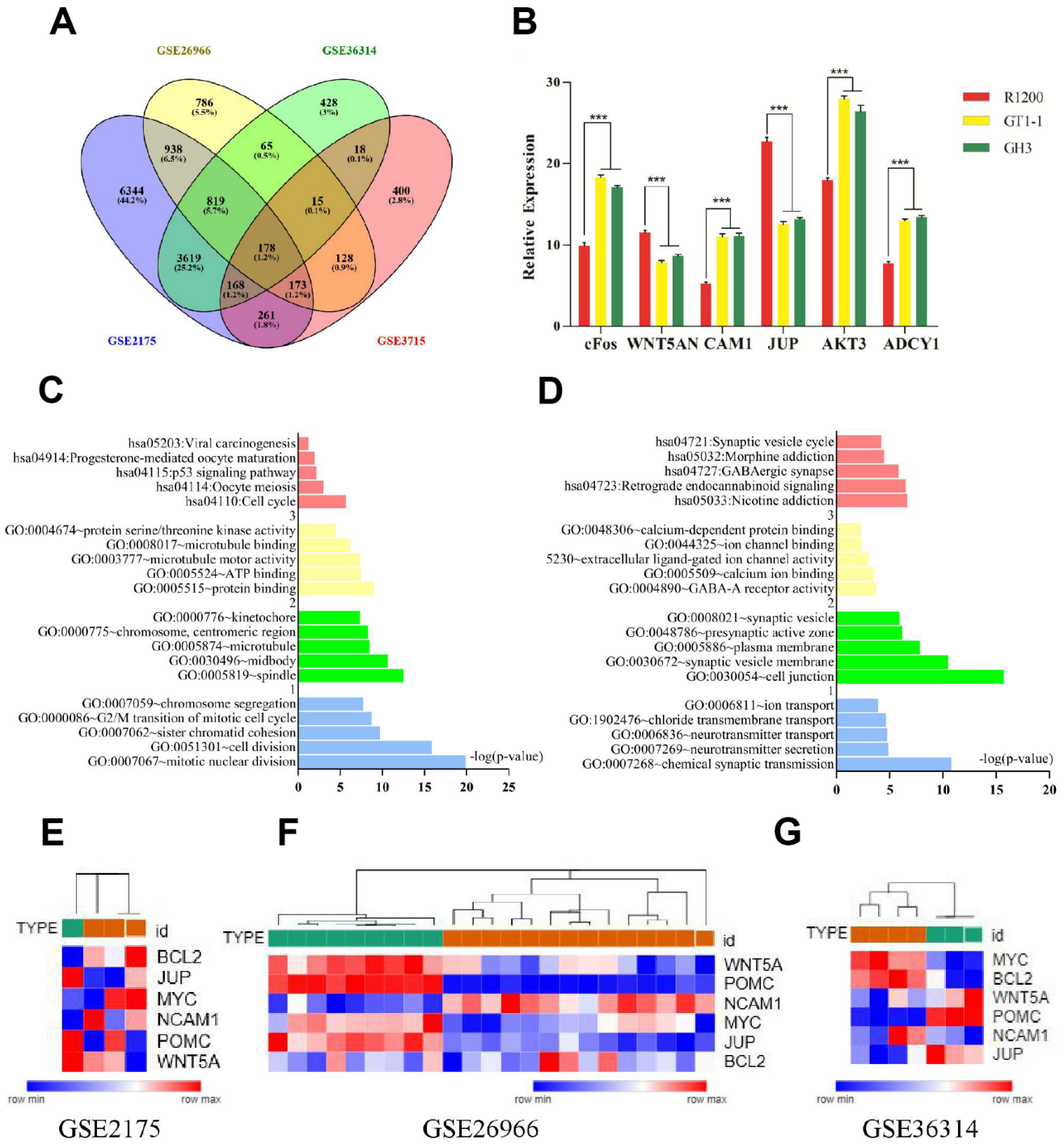

Figure 1. (**A**) Venn diagrams for DEGs. **(B)** Results of q-PCR analysis. (**C**) Functional and pathway enrichment analysis of up- regulated genes. (**B**) Expression heat map of hub genes. (**D**) Functional and pathway enrichment analysis of down-regulated genes. (**E**–**G**) Expression heat map of hub genes.

Table 1. Functional and pathway enrichment analysis of up-regulated and down-regulated genes among four datasets.

Expression	Category	Term	Count	%	P Value
up-regulated	GOTERM_BP_DIRECT	GO:0007067~mitotic nuclear division	18	38.29787234	1.28E-20
	GOTERM_BP_DIRECT	GO:0051301~cell division	17	36.17021277	1.39E-16
	GOTERM_BP_DIRECT	GO:0007062~sister chromatid cohesion	9	19.14893617	1.85E-10
	GOTERM_BP_DIRECT	GO:0000086~G2/M transition of mitotic cell cycle	9	19.14893617	1.82E-09
	GOTERM_BP_DIRECT	GO:0007059~chromosome segregation	7	14.89361702	1.91E-08
	GOTERM_CC_DIRECT	GO:0005819~spindle	11	23.40425532	2.99E-13
	GOTERM_CC_DIRECT	GO:0030496~midbody	10	21.27659574	2.40E-11
	GOTERM_CC_DIRECT	GO:0005874~microtubule	11	23.40425532	3.41E-09
	GOTERM_CC_DIRECT	GO:0000775~chromosome, centromeric region	7	14.89361702	5.29E-09
	GOTERM_CC_DIRECT	GO:0000776~kinetochore	7	14.89361702	4.53E-08
	GOTERM_MF_DIRECT	GO:0005515~protein binding	41	87.23404255	9.05E-10
	GOTERM_MF_DIRECT	GO:0005524~ATP binding	18	38.29787234	3.45E-08
	GOTERM_MF_DIRECT	GO:0003777~microtubule motor activity	7	14.89361702	4.29E-08
	GOTERM_MF_DIRECT	GO:0008017~microtubule binding	8	17.0212766	7.29E-07
	GOTERM_MF_DIRECT	GO:0004674~protein serine/threonine kinase activity	8	17.0212766	3.54E-05
	KEGG_PATHWAY	hsa04110:Cell cycle	6	12.76595745	1.97E-06
	KEGG_PATHWAY	hsa04114:Oocyte meiosis	4	8.510638298	9.73E-04
	KEGG_PATHWAY	hsa04115:p53 signaling pathway	3	6.382978723	0.00674313
	KEGG_PATHWAY	hsa04914:Progesterone-mediated oocyte maturation	3	6.382978723	0.01117001
	KEGG_PATHWAY	hsa05203:Viral carcinogenesis	3	6.382978723	0.05510903
down-regulated	GOTERM_BP_DIRECT	GO:0007268~chemical synaptic transmission	16	14.15929204	1.58E-11
	GOTERM_BP_DIRECT	GO:0007269~neurotransmitter secretion	6	5.309734513	1.41E-05
	GOTERM_BP_DIRECT	GO:0006836~neurotransmitter transport	5	4.424778761	1.73E-05
	GOTERM_BP_DIRECT	GO:1902476~chloride transmembrane transport	7	6.194690265	2.15E-05
	GOTERM_BP_DIRECT	GO:0006811~ion transport	7	6.194690265	1.24E-04
	GOTERM_CC_DIRECT	GO:0030054~cell junction	25	22.12389381	1.97E-16
	GOTERM_CC_DIRECT	GO:0030672~synaptic vesicle membrane	10	8.849557522	3.25E-11
	GOTERM_CC_DIRECT	GO:0005886~plasma membrane	52	46.01769912	1.47E-08
	GOTERM_CC_DIRECT	GO:0048786~presynaptic active zone	6	5.309734513	7.06E-07
	GOTERM_CC_DIRECT	GO:0008021~synaptic vesicle	8	7.079646018	1.22E-06
	GOTERM_MF_DIRECT	GO:0004890~GABA-A receptor activity	4	3.539823009	1.88E-04
	GOTERM_MF_DIRECT	GO:0005509~calcium ion binding	14	12.38938053	3.42E-04
	GOTERM_MF_DIRECT	GO:0005230~extracellular ligand-gated ion channel activity	4	3.539823009	9.96E-04
	GOTERM_MF_DIRECT	GO:0044325~ion channel binding	5	4.424778761	0.00472253

GOTERM_MF_DIRECT	GO:0048306~calcium-dependent protein binding	4	3.539823009	0.00505404
KEGG_PATHWAY	hsa05033:Nicotine addiction	7	6.194690265	2.30E-07
KEGG_PATHWAY	hsa04723:Retrograde endocannabinoid signaling	9	7.96460177	3.09E-07
KEGG_PATHWAY	hsa04727:GABAergic synapse	8	7.079646018	1.40E-06
KEGG_PATHWAY	hsa05032:Morphine addiction	7	6.194690265	3.07E-05
KEGG_PATHWAY	hsa04721:Synaptic vesicle cycle	6	5.309734513	6.13E-05

Table 2. Detailed information of the hub genes among four datasets.

Gene symbol	Degree	Betweenness centrality	Gene symbol	Degree	Betweenness centrality
cFos	22	0.3840231	GH1	6	0.01536337
MYC	20	0.3150368	CCND2	6	0.02628263
WNT5A	18	0.1803458	TSHB	6	0.01756622
BCL2	17	0.37660255	GHRHR	6	0.00112801
NCAM1	13	0.24487191	PPP2R5A	6	0.11767315
JUP	12	0.0401026	BCR	6	0.03518683
POMC	11	0.05597786	CAMK2G	6	0.03972707
AKT3	10	0.03310717	ATP2A2	6	0.12136994
ADCY1	9	0.00765123	APC	5	0.02201292
FGFR2	7	0.0745872	MAD2L1	5	0.07012635

cellular viability (ratio to controls) in cell lines GT1-1 and GH3 dropped, decreasing more rapidly for T5224 than for STO609, Genipin ($P < 0.05$), RSPO2, and AZD5363. Besides, compared to STO609, cellular viability also declined faster for Genipin in cell line GT1-1. However, in GH3 cells, cellular viability was similar for STO609 and Genipin.

Colony-formation assays revealed different percentages of clone formation for each drug treatment group. Compared to controls, there were fewer and smaller colonies in all drug groups (0.5μmol/L, 1μmol/L). On the other hand, clonogenicities were approximately the same for the STO609 and Genipin groups, both of which were higher than those for the T5224, RSPO2, and AZD5363 groups ($P < 0.05$) (Figure 5). Higher drug concentrations correlated with fewer clonogenicities, implying dose-dependent effects for T5224, RSPO2, and AZD5363.

T5224, RSPO2, and AZD5363 induce apoptosis of FPA cells

Flow cytometry of FPA cells and controls treated with different doses of drugs for 48 h allowed us to measure the percentages of normal, necrotic, late apoptotic, and early apoptotic cells. For controls, the respective percentages were 57.35%, 16.04%, 21.33%, and 5.28%. On the other hand, for T-5224-treated cells they were 5.69%, 1.08%, 59.74%, and 33.49% in low-dose group (10 μmol/L); 0.36%, 0.55%, 70.23%, and 28.86% in the intermediate-dose group (20 μmol/L); and 0.16%, 0.91%, 83.13%, and 15.8% in the high-dose group (40 μmol/L) (Figure 6A). For STO-609-treated cells, the numbers were 13.37%, 1.73%, 34.72%, and 50.17% in the low-dose group (35 μmol/L); 12.29%, 2.93%, 60.1%, and 24.68% in the middle-dose group (75 μmol/L); and 4.04%, 3.01%, 79.71%, and 13.24% in the high-dose group (150 μmol/L) (Figure 6B). The relevant numbers for Genipin were 0.23%, 1.08%, 97.28%, 1.41% in low dose group (75 μmol/L) and 0.22%, 0.51%, 90.53%, 8.74% in high dose group (150 μmol/L) (Figure 7A). For RSPO2-treated cells, the percentages were 7.19%, 4.15%, 48.04%, and 40.62% in the low-dose group (75 μmol/L), and 1.72%, 6.59%, 90.72%, and 0.97% in the high-dose group (150 μmol/L) (Figure 7B). For AZD5363-treated cells, the percentages were 6.91%, 3.75%, 52.22%, and 37.12% in the low-dose group (75 μmol/L), and 0.24%, 0.71%, 97.32%, and 1.73% in the high-dose group (150 μmol/L) (Figure 7C). We noticed that normal cells were predominant in the control group while apoptotic cells were predominant in the presence of T5224, RSPO2, or AZD5363 treatment. Compared to STO-609-treated cells, there was a greater percentage of apoptotic cells in the T5224, Genipin, RSPO2, and AZD5363-treated groups, even when using the same dose for all drugs.

DISCUSSION

Many FPA patients present reduced quality of life, persistent morbidity, and slightly increased mortality in spite of receiving current therapies [4]. In the present study, we analyzed the gene expression profiles of 21 FPA samples and 14 normal samples from mRNA microarray datasets GSE2175, GSE26966, GSE36314, and GSE37153 in the GEO database. And a total of 19,943, 4635, 6472, and 2020 DEGs were identified respectively from those four datasets. There were 178 "mutual DEGs" identified by performing Venn plot among those four datasets.

GO analysis of abnormally expressed genes showed that upregulated genes were mainly associated with biological processes relevant to mitotic proliferation such as cell division, spindle formation, microtubule polymerization, protein binding, and ATP binding, which may explain the fast multiplication of cancer cells. Downregulated genes were primarily involved in biological processes underlying cell communication and signaling, including ion transport, cell junction and plasma membrane formation, calcium-dependent protein binding and calcium ion binding. Our results agree with a previous study showing that over-representation of genes can modify the course of the cell cycle, cell development, and

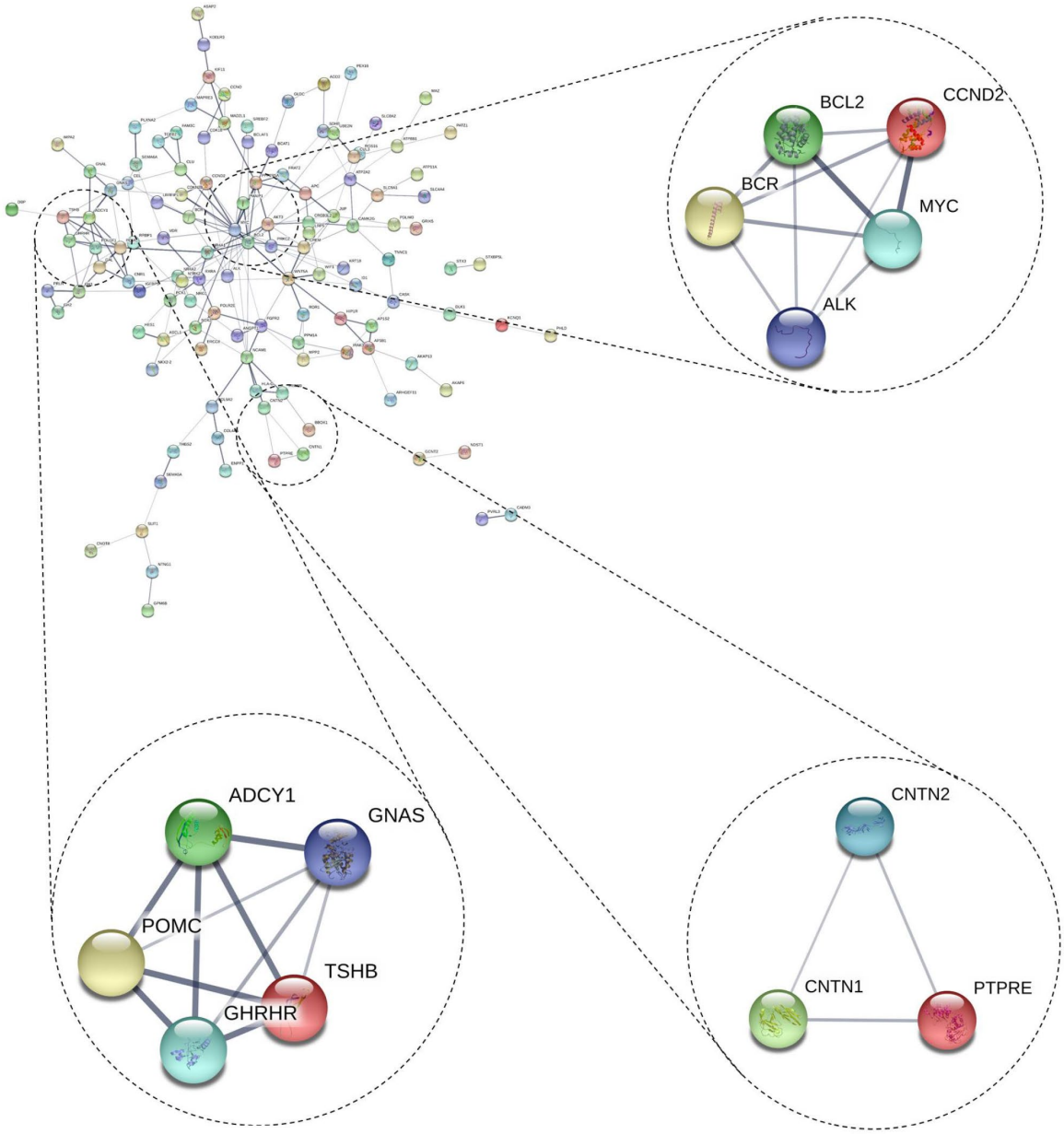

Figure 2. Top 3 modules from the protein-protein interaction network.

Table 3. Functional and pathway enrichment analysis of the modules genes.

Module	Term	Count	P Value	FDR	Genes
module 1	GO:0008283~cell proliferation (BP)	3	2.76E-03	3.48761792	BCL2, ALK, MYC
	GO:0043234~protein complex (CC)	3	2.97E-03	2.382996199	BCR, ALK, MYC
	GO:0043066~negative regulation of apoptotic process (BP)	3	4.24E-03	5.307949002	CCND2, BCL2, MYC
module 2	GO:0007190~activation of adenylate cyclase activity(BP)	3	3.31E-05	3.62E-02	ADCY1, GNAS, GHRHR
	GO:0007189~adenylate cyclase-activating G-protein coupled receptor signaling pathway(BP)	3	5.19E-05	5.67E-02	ADCY1, GNAS, GHRHR
	hsa04923:Regulation of lipolysis in adipocytes(KEGG)	3	3.83E-04	3.72E-01	ADCY1, TSHB, GNAS
module 3	GO:0001948~glycoprotein binding(MF)	2	7.69E-03	3.89981344	CNTN2, CNTN1
	GO:0031225~anchored component of membrane(CC)	2	1.24E-02	8.45522442	CNTN2, CNTN1
	GO:0043209~myelin sheath(CC)	2	1.66E-02	11.21564142	CNTN2, CNTN1

cell differentiation/proliferation in pathologic adenoma cells [11]. Several studies have also shown that cell membrane ion channels, especially potassium channels, participate in cell signal transduction, proliferation, apoptosis, and regulation of gene expression in tumors [12]. Furthermore, the KEGG analyses we conducted here revealed that the mutual DEGs were mainly involved in the cell cycle, the p53 signaling pathway, oocyte meiosis, nicotine addiction, GABAergic synapse, and morphine addiction.

The levels of some cell-cycle regulators (p16, pRB protein, and cyclin D1) can predict the occurrence and proliferation of FPA [13]. The P53 signaling pathway is involved in cell cycle arrest, apoptosis, senescence, DNA repair, and changes in metabolism [14]. Thus, it is not surprising that P53 mutations are the most common in malignant tumors. The inhibition of p53 caused by c-Jun upregulation promotes FPA invasion [15]. Also, morphine promotes tumor growth by inhibiting apoptosis and promoting angiogenesis and migration of tumor cells [16]. Similarly, tobacco compounds have long been known to promote cell proliferation [17], suggesting that smoking may increase the probability of developing FPA.

c-Fos, one of the components of the activator protein-1 (AP-1) transcription factors, is hyper-activated in tumorigenesis and promotes cancer cell invasion and proliferation [18–19] for various types of cancer (Table 4) [18–20]. Injection treatment with FGFR1 inhibitor AZD4547 decreases the number and surface area of metastatic lung nodules and parenchyma in mice [21], highlighting AZD4547 as a potential treatment for other types of cancer. Similarly, T5224 inhibits AP-1, c-Fos, and therefore FGFR1, which suggests that it might exert anti-FPA effects.

WNT5A promotes malignant progression in tumor cells [22–23] and is overexpressed in many types of cancer [22–24] (Table 4). RSPO2 inhibits tumor cell migration [49], implying it might also have therapeutic effects in FPA.

NCAM1 is a neural cell adhesion molecule that promotes cell-cell and cell-matrix interactions during development and cellular differentiation [25]. NCAM1 promotes other normal cellular processes [26] and genes in the underlying pathways are more likely to be deregulated in tumors that have migrated to lymph nodes, especially basal-like tumors associated with poor prognosis [25]. NCAM1 is also deregulated in other types of cancer (Table 4) [27], which suggests it might serve as a prognostic biomarker and therapeutic target for FPA [28–29].

The junction plakoglobin gene (JUP) is a desmosomal anchor protein gene, whose normal functioning is necessary for having healthy inter-cellular junctions and microtubules [30–31]. JUP is abnormally expressed in

various diseases, including cancer (Table 4) [30–33], and its overexpression promotes metastasis and primary site recurrence in squamous cell carcinoma [34–35]; thus, JUP levels might also inform on the recurrence of FPA.

Protein kinase AKT3 promotes progression, metastasis, and drug resistance in various types of cancer (Table 4) [36–39]. AZD5363, a Akt3 inhibitor, inhibits proliferation in prostate cancer [50], which suggests it could also have therapeutic effects in in FPA.

ADCY1, adenylate cyclase 1, catalyzes the synthesis of cAMP [40–41] and was found to be dysregulated in rectal adenocarcinoma (RAC) and other cancers (Table 4)

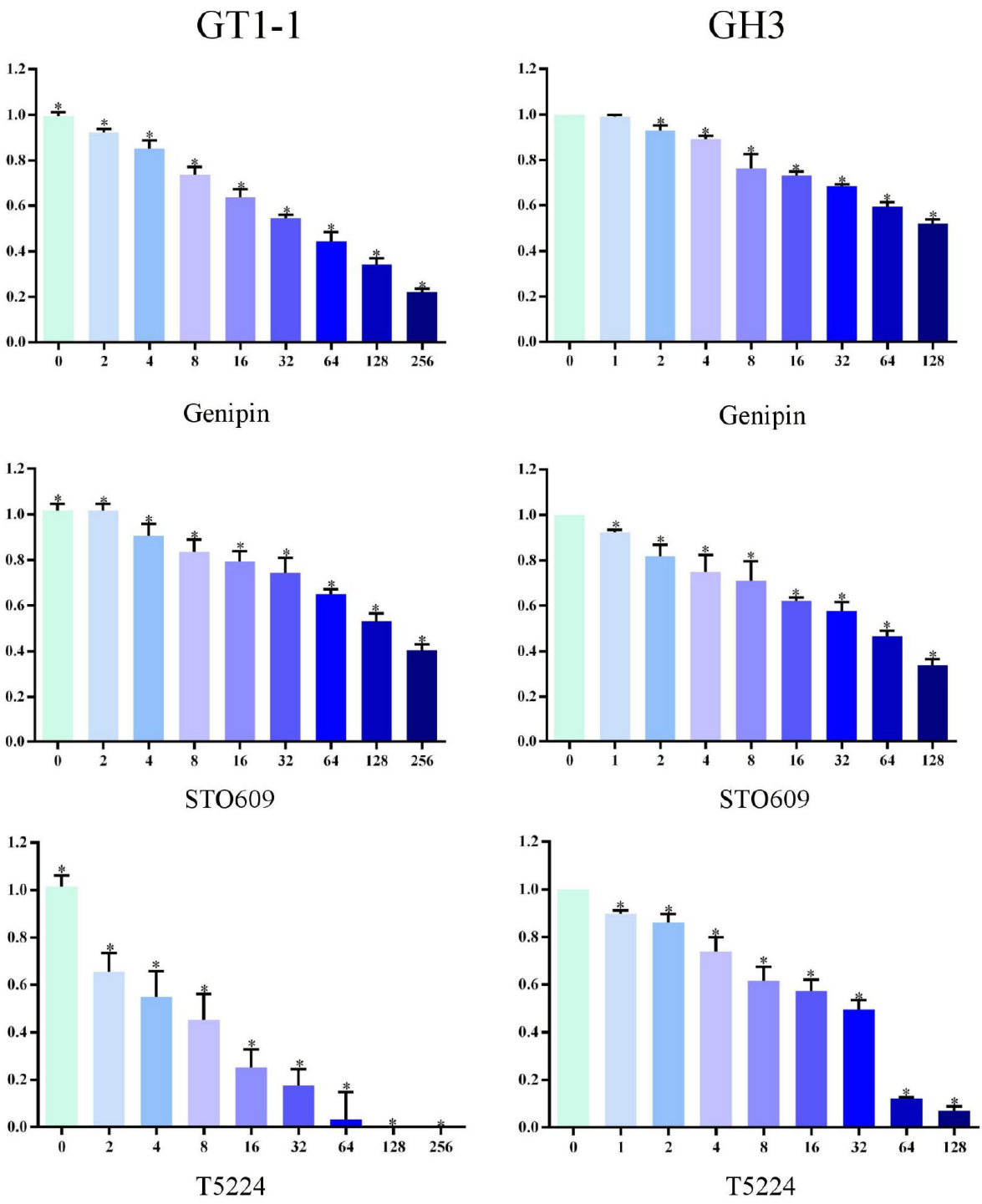

Figure 3. Cellular viability of glioblastoma cells treated with T5224, Genipin and STO-609.

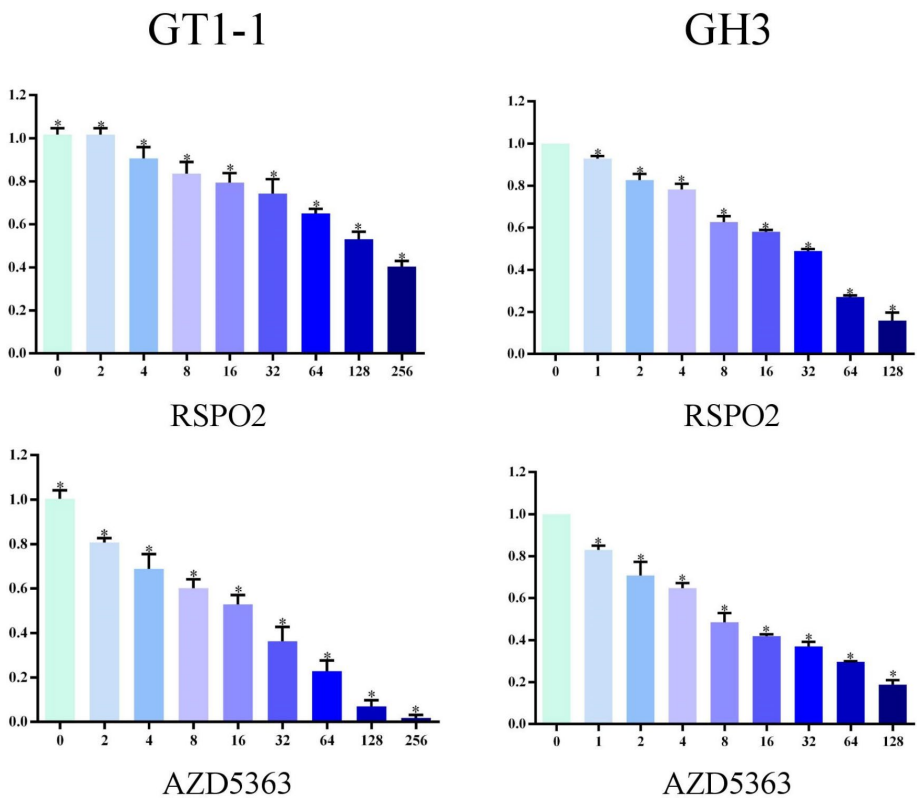

Figure 4. Cellular viability of glioblastoma cells treated with RSPO2 and AZD5363.

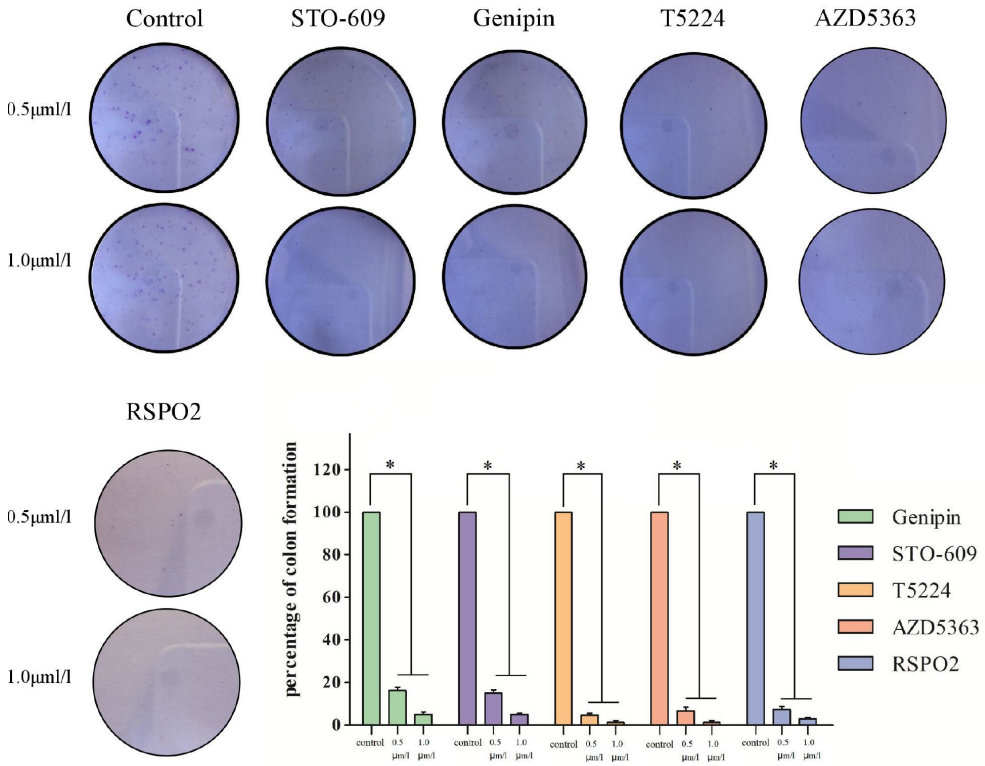

Figure 5. Clonogenicities in Petri dishes with different dose of T5224, RSPO2, AZD5363, Geinpin, and STO-609.

[40, 42]. In addition, ADCY1 overexpression promotes multi drug-resistant esophageal carcinoma-1 [43]. Fortunately, ADCY1 target drugs improve prognosis for esophageal carcinoma patients, which suggests that these drugs may also help FPA patients [43–44].

In this study, cFos, NCAM1, JUP, AKT3 ADCY1, CCND2, PPP2R5A, CAMK2G, ATP2A2, and MAD2L1 as well as hub genes were shown to be dysregulated in FPA and may serve as therapeutic targets or prognostic and diagnostic makers.

We used qRT-PCR to measure cFos, WNT5A, NCAM1, JUP, AKT3, and ADCY1 levels in normal pituitary cells (R1200) and FPA cell lines (GT1-1, GH3). We found that the expression of cFos, NCAM1, AKT3, and ADCY1 was lower in normal pituitary cells than in FPA cells ($P < 0.05$) while WNT5A and JUP levels were

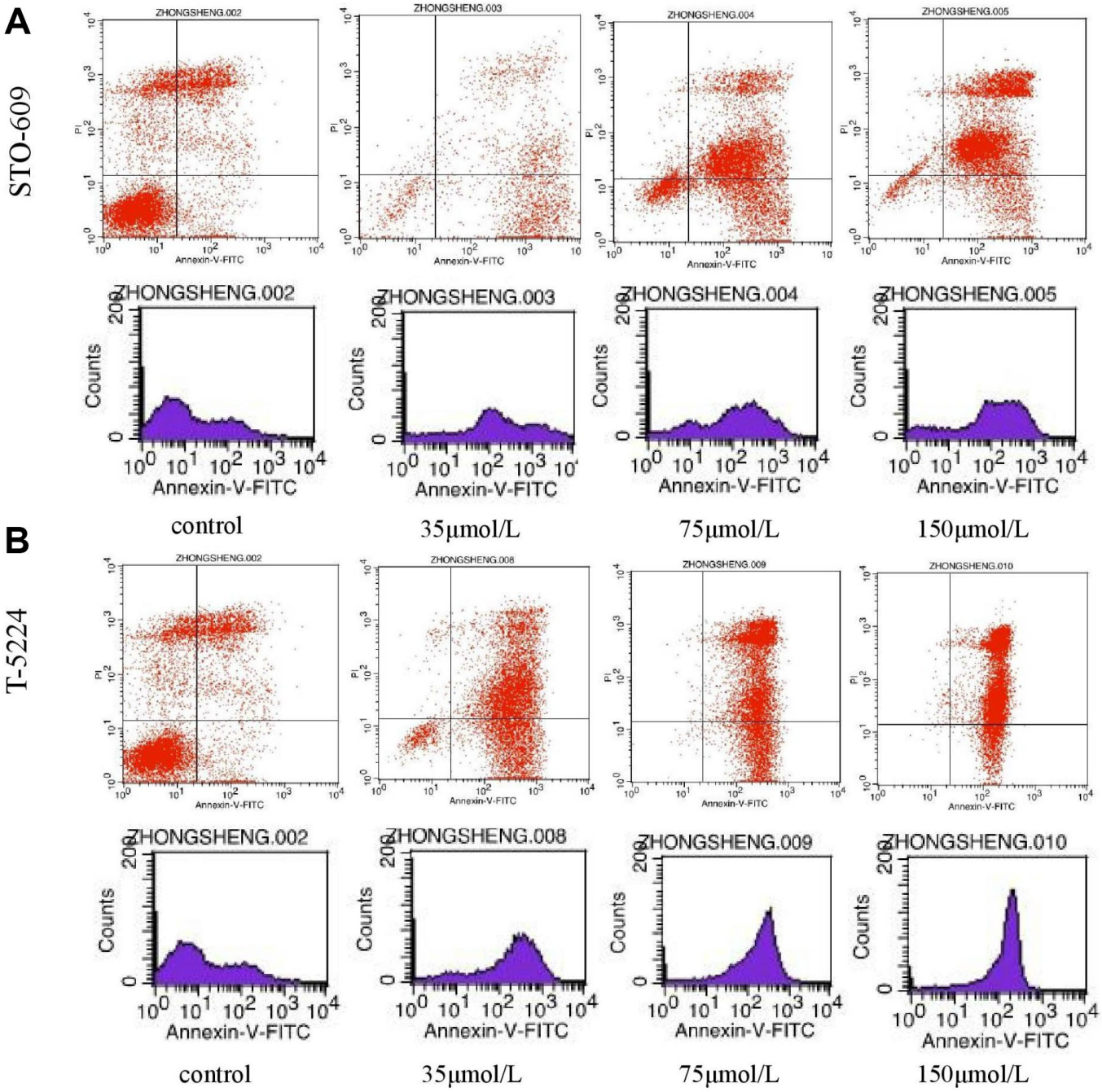

Figure 6. The distribution of cells in apoptosis with different doses of (**A**) STO-609 and (**B**) T5224.

higher. This means that high expression of cFos, NCAM1, AKT3, and ADCY1 promotes tumorigenesis while high levels of AKT3 and ADCY1 inhibits it.

We used MTT and colony-formation assays to evaluate the effects of T5224, RSPO2, and AZD5363 on FPA. For cell lines GT-1 and GH3, cell viability correlated negatively with T5224, RSPO2, AZD5363, STO-609, and Genipin treatments in a dose-dependent manner. Furthermore, the ratio of T5224 groups dropped more significantly than the rest of groups in GH1-1 cell lines, including RSPO2 and AZD5363 groups. That indicates that T5224, RSPO2, and AZD5363 have therapeutic effects on FPA cells and protective effects on normal pituitary cells. Similarly, colony-forming assays showed that the number and size of clonogenicities in the drug groups were remarkably smaller than in controls and correlating negatively with treatment in a dose-dependent manner, with T5224, RSPO2, and AZD5363 yielding the smallest clonogenicities, in agreement with the results of our MTT assays.

Our flow cytometry experiments on FPA cells treated with different doses of T5224, RSPO2, AZD5363, STO-609, or Genipin for 48 h, showed that apoptosis correlated positively with treatment dose in all five drug groups compared to controls, suggesting beneficial effects from such drugs in the treatment of FPA.

Considering previous studies, the results of our *in vitro* study here indicate that T5224 exerts anti-FPA effects specifically by inhibiting cFos pathways and that RSPO2 does so by inhibiting Wnt5A while AZD5363 inhibits Akt3. Further studies *in vivo* should be conducted to test the therapeutic effects we uncovered here in more clinically-relevant systems.

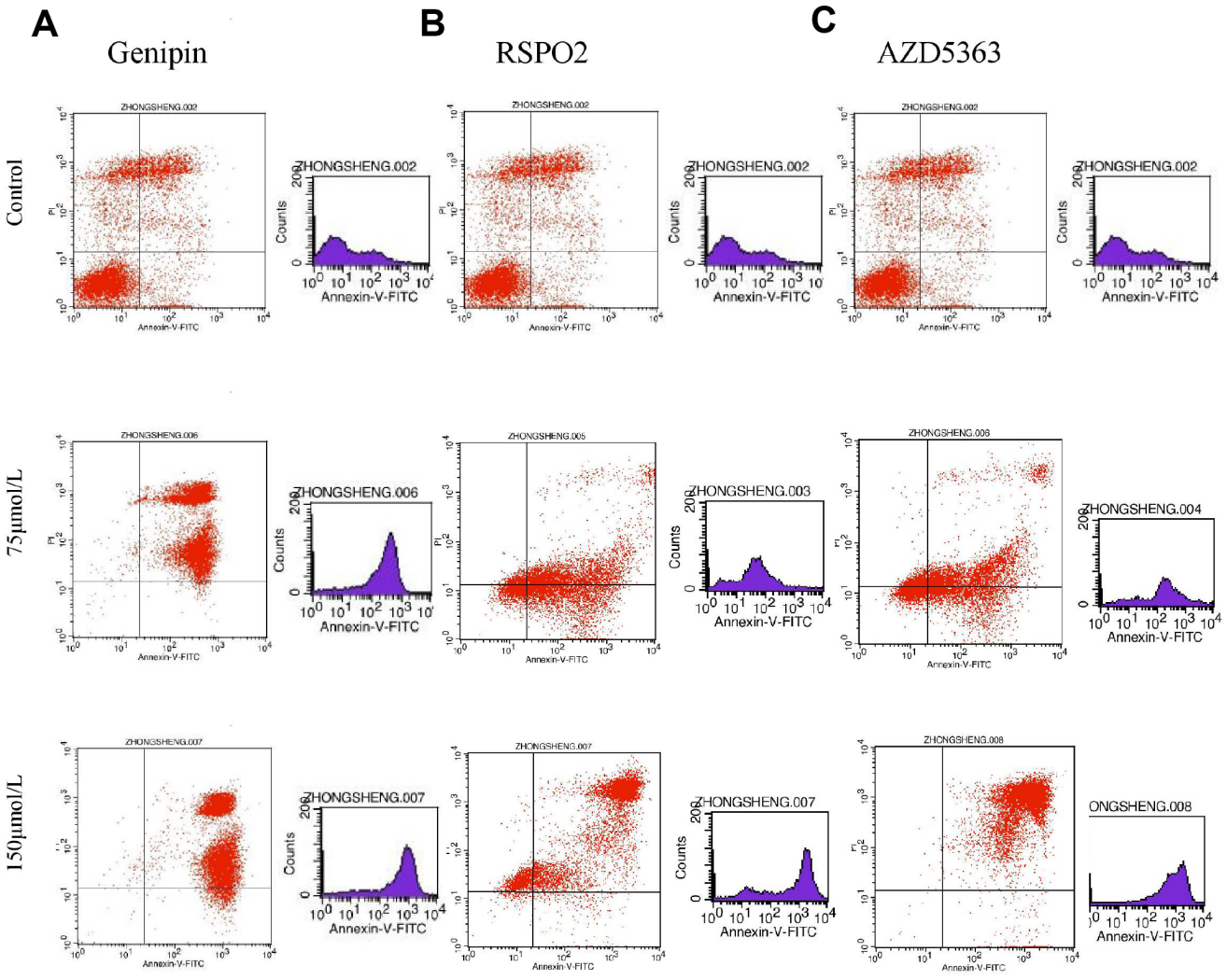

Figure 7. The distribution of cells in apoptosis with different dose of (**A**) Genipin, (**B**) RSPO2, and (**C**) AZD5363.

Table 4. Hub genes and related cancers.

Hub genes	Related cancers
c-Fos	breast cancer, osteosarcoma, endometrial carcinoma, bladder cancer, prostate cancer, hepatoma cancer, et al.
WNT5A	prostate cancer, melanoma, gastric carcinoma, breast cancer, prostate cancer, lung metastasis of sarcoma cells, et al.
NCAM1	ovarian carcinoma, gastric cancer, melanoma, Wilms tumor (WT), et al.
JUP	colorectal cancer, oral intraepithelial neoplasms, breast cancer, serous ovarian cancer, testicular cancer, et al.
AKT3	glioma, breast cancer, leukemia, colon cancer and prostate cancer, et al.
ADCY1	esophageal carcinoma, pancreatic cancer, rectal adenocarcinoma, et al.

MATERIALS AND METHODS

Microarray data

The gene expression profiles of GSE2175, GSE26966, GSE36314, and GSE37153 were obtained from the GEO database (https://www.ncbi.nlm.nih.gov/geo). The corresponding profiles were provided on platform GPL96 (GSE2175), GPL570 (GSE26966), GPL8300 (GSE36314), and GPL6480 (GSE37153) [45–48]. The GSE2175 contained one FPA samples and three normal samples, 14 FPA tissues and nine normal samples in the GSE26966. The GSE36314 provided four FPA samples and three normal pituitary tissues, and GSE37153 consisted of two FPA samples and one normal sample.

Identification of DEGs

Analyses of the raw data were carried out using GeneSpring software (version 11.5, Agilent, USA) for four groups of DEGs to fit four respective gene expression profiles. The category of each data set was derived from hierarchical clustering. Group FPA and normal tissues were identified. The probe quality control in GeneSpring was limited by virtue of principal component analysis (PCA), and probes with intensity values below the 20th percentile were filtered out using the "filter probesets by expression" option. Then, the DEGs were identified using classical *t* test with P value cutoff of < 0.05 and a change $\geq$ two fold. We also computed Venn diagrams for each DEG (http://bioinformatics.psb.ugent.be/webtools/Venn/).

Gene ontology and pathway enrichment analysis of DEGs

The DAVID database (Database for Annotation, Visualization and Integrated Discovery, https://david.ncifcrf.gov/) provides a comprehensive annotation tools to understand the biological meaning underlying plenty of genes. GO (Gene Ontology) is a useful method for exposing biological process, molecular function, and cell component of genes. KEGG (Kyoto encyclopedia of Genes and Genomes) is a base for gene function analysis and genomic information linking. We performed GO and KEGG pathway enrichment analyses using DAVID for functional analyses of DEGs.

PPI network construction and modules selection

We used the online database STRING (Search Tool for Retrieval of Interacting Genes, https://string.embl.de/) for PPI (Protein-Protein interaction) analysis. Then, we used Cytoscape software to screen hub genes and modules with MCODE (Molecular Complex Detection). Finally, we performed function and pathway enrichment analyses of DEGs in modules.

Cell lines

Normal pituitary cells (R1200) and FPA cells (GT1-1 and GH3) were received from the ATCC (American Type Culture Collection). Those cell lines were cultured in Dulbecco's modified Eagle's medium (DMEM, Hyclone, USA) supplemented with 10% fetal bovine serum (FBS, Gibco, USA). The cell cultures were maintained at 5% CO_2 and 95% air at 37 °C.

Real-time quantitative reverse transcription PCR

To verify the expression of cFos, WNT5A, NCAM1, JUP, AKT3, and ADCY1 in FPA cell lines and normal human pituitary cells, we used FastStart Universal SYBR Green Master (ROX) (Roche Diagnostics) to perform qRT-PCR in a CFX96 Real-Time System (Bio-Red) according to the manufacturer's instructions. Expression levels were normalized to glyceraldehyde-3-phosphate dehydrogenase (GAPDH). The $2^{-\Delta\Delta Ct}$ method was used for qRT-PCR data analysis. The primers of genes were enumerated as followed: cFos sense, 5′-CCTCTCCATGCAGGAGTTAAGA-3′; cFos anti-sense, 5′-GGTCTCGGGTCCTTGATTTTCT-3′; WNT 5A sense, 5′-TACTGCGGTGGAGCAAGAAG-3′; WNT5A anti-sense, 5′-CATCTGCGCTTGACGGAGA G-3′; NCAM1 sense, 5′-AGCCCATCAATAAGGGAG GG-3′; NCAM1 anti-sense, 5′-ACCTGACACCCGTTT

TAGCTG-3′; JUP sense, 5′-TACTGCGGTGGAGCAA GAAG-3′; JUP anti-sense, 5′-CATCTGCGCTTGACG GAGAG-3′; ADCY1 sense, 5′-TACTGCGGTGGAGC AAGAAG-3′; ADCY1 anti-sense, 5′-CATCTGCGCTT GACGGAGAG-3′.

MTT assay

The FPA cells (GT1-1, GH3) were plated into 96-well culture plate with a density of 500 cells/well, and were treated with different doses of T-5224, RSPO2, and AZD5363, respectively, as well as STO-609 (CaMKK inhibitor) and Genipin (aglycone derived from the iridoid glycoside), both of which protect against several types of tumors, including brain tumors. We used MTT (Sigma, St. Louis, Missouri, USA) dissolved in PBS (5 mg/ml) to measure the viability of cells. On the day of measurement, the medium was replaced on fresh DMEM supplemented with 10% FBS and diluted MTT (1:10, 10% MTT), and incubated for 3.5 h at 37 °C. Then, the incubation medium was removed and formazan crystals were dissolved in 200 μl solution of DMSO. We used an ELx800 absorbance microplate reader (BioTek Instruments, VT, USA) to quantify the MTT reduction by measuring light absorbance at 570 nm. Each test was repeated four times.

Colony-forming assay

FPA cells (GT1-1, GH3) were seeded in Petri dishes with a density of 50 cells/cm^2. After 24 h in culture, the cells were treated with different doses of STO-609, Genipin, T-5224, RSPO2, and AZD5363, respectively. After 10 days of growth *in vitro*, colonies were counted and described according to Franken et al. Then, colonies were rinsed with PBS, fixed in 4% paraformaldehyde, stained with 5% crystal violet for 0.5 h, and rinsed twice with water.

Flow cytometry

The FPA cells (GT1-1) in the log growth phase were seeded into 6-well plates with a density of 2×10^5 cells/well and treated with different doses of STO-609, Genipin, T-5224, RSPO2 and AZD5363. After 48 h of culturing, the cells were harvested using accutase detachment solution (Sigma Aldrich, USA). Annexin-V-FITC/PI labeling was conducted according to the manufactures' instruction. a flow cytometer was used to count stained cells with the FACSDiva Version 6.2.

Statistics

All statistical data analyses were carried out using SPSS 18.0 (SPSS Inc., Chicago, Illinois, USA), namely *t* tests for independent samples with P values < 0.05.

Abbreviations

ATCC: American Type Culture Collection; ACTH: Adrenocorticotropic; AP-1: Activator protein-1; ADCY1: Adenylate cyclase 1; BP: Biological processes; BMP: Bone morphogenetic proteins; CC: Cell component; DEG: Differential expressed genes; DAVID: Database for Annotation, Visualization and Integrated Discovery; DMEM: Dulbecco's modified Eagle's medium; Eca-1: Esophageal carcinoma-1; FBS: Fetal bovine serum; FPA: Functioning pituitary adenomas; GO: Gene ontology; GH: Growth hormone; GEO: Gene Expression Omnibus; miRNAs: HMGA-targeting microRNAs; JUP: Junction plakoglobin,; KEGG: Kyoto encyclopedia of Genes and Genomes; LN1: Lymph node-positive; MF: Molecular function; nAChRs: Nicotinic acetylcholine receptors; NCAM1: Neural Cell Adhesion Molecule; PRL: Prolactinoma; PA: Pituitary adenomas; PKB: Protein kinase B; PCA PCA: Principal component analysis; PPI: Protein-protein interaction; RAC: Rectal adenocarcinoma; STRING: Search Tool for Retrieval of Interacting Genes; TSH: Thyroid-stimulating hormone; WHO: World Hearth Organization; WNT5A: Wnt member 5a; WT: Wilms' tumor; β-ARs: β-Adrenergic receptors.

AUTHOR CONTRIBUTIONS

Sheng Zhong and Bo Wu designed experiments; Jiahui Li and Xinhui Wang wrote the manuscript. Shanshan Jiang, Fangfei Hu, Gaojing Dou carried out experiments; Yuan Zhang Chunjia Sheng analyzed experimental results. Yong Chen analyzed sequencing data.

CONFLICTS OF INTEREST

The authors declare no conflicts of interest.

FUNDING

This study was supported by grants from the National Natural Science Foundation of China (Nos. 81672505 and 81772684), the S&T Development Planning Program of Jilin Province (Nos. 20160101086JC, 20160312017ZG, and 20180101152JC), the Jilin Provincial Education Department "13th Five-Year" Science and Technology Project (JJKH20180191KJ) and the Interdisciplinary Innovation Project of The First Hospital of Jilin University (JDYYJC001).

REFERENCES

1. Kim JW, Kim DG. Stereotactic radiosurgery for functioning pituitary adenomas. World Neurosurg. 2014; 82:58–59.

https://doi.org/10.1016/j.wneu.2013.03.015
PMID:23500123

2. Lake MG, Krook LS, Cruz SV. Pituitary adenomas: an overview. Am Fam Physician. 2013; 88:319–27. PMID:24010395

3. Aflorei ED, Korbonits M. Epidemiology and etiopathogenesis of pituitary adenomas. J Neurooncol. 2014; 117:379–94. https://doi.org/10.1007/s11060-013-1354-5 PMID:24481996

4. Pereira AM. Long-term effects of treatment of pituitary adenomas. Handb Clin Neurol. 2014; 124:361–71. https://doi.org/10.1016/B978-0-444-59602-4.00024-1 PMID:25248599

5. Glezer A, Bronstein MD. Prolactinoma. Arq Bras Endocrinol Metabol. 2014; 58:118–23. https://doi.org/10.1590/0004-2730000002961 PMID:24830588

6. Loyo-Varela M, Herrada-Pineda T, Revilla-Pacheco F, Manrique-Guzman S. Pituitary tumor surgery: review of 3004 cases. World Neurosurg. 2013; 79:331–36. https://doi.org/10.1016/j.wneu.2012.06.024 PMID:22732515

7. Palmieri D, D'Angelo D, Valentino T, De Martino I, Ferraro A, Wierinckx A, Fedele M, Trouillas J, Fusco A. Downregulation of HMGA-targeting microRNAs has a critical role in human pituitary tumorigenesis. Oncogene. 2012; 31:3857–65. https://doi.org/10.1038/onc.2011.557 PMID:22139073

8. Duong CV, Yacqub-Usman K, Emes RD, Clayton RN, Farrell WE. The EFEMP1 gene: a frequent target for epigenetic silencing in multiple human pituitary adenoma subtypes. Neuroendocrinology. 2013; 98:200–11. https://doi.org/10.1159/000355624 PMID:24080855

9. Yacqub-Usman K, Duong CV, Clayton RN, Farrell WE. Epigenomic silencing of the BMP-4 gene in pituitary adenomas: a potential target for epidrug-induced re-expression. Endocrinology. 2012; 153:3603–12. https://doi.org/10.1210/en.2012-1231 PMID:22700770

10. Ye N, Ding Y, Wild C, Shen Q, Zhou J. Small molecule inhibitors targeting activator protein 1 (AP-1). J Med Chem. 2014; 57:6930–48. https://doi.org/10.1021/jm5004733 PMID:24831826

11. Lee M, Marinoni I, Irmler M, Psaras T, Honegger JB, Beschorner R, Anastasov N, Beckers J, Theodoropoulou M, Roncaroli F, Pellegata NS. Transcriptome analysis of MENX-associated rat pituitary adenomas identifies novel molecular mechanisms involved in the pathogenesis of human pituitary gonadotroph adenomas. Acta Neuropathol. 2013; 126:137–50. https://doi.org/10.1007/s00401-013-1132-7 PMID:23756599

12. Wu S, Gu Y, Huang Y, Wong TC, Ding H, Liu T, Zhang Y, Zhang X. Novel Biomarkers for Non-functioning Invasive Pituitary Adenomas were Identified by Using Analysis of microRNAs Expression Profile. Biochem Genet. 2017; 55:253–67. https://doi.org/10.1007/s10528-017-9794-9 PMID:28315020

13. Tittensor DP. Biodiversity: temperate hotspots. Nature. 2013; 501:494–95. https://doi.org/10.1038/501494a PMID:24067706

14. Yan J, Zhang F, Huang Q. FTIR Microspectroscopy Probes Particle-Radiation Effect on HCT116 cells ($p53^{+/+}$, $p53^{-/-}$). Radiat Res. 2018; 189:156–64. https://doi.org/10.1667/RR14883.1 PMID:29206599

15. Kamide D, Yamashita T, Araki K, Tomifuji M, Tanaka Y, Tanaka S, Shiozawa S, Shiotani A. Selective activator protein-1 inhibitor T-5224 prevents lymph node metastasis in an oral cancer model. Cancer Sci. 2016; 107:666–73. https://doi.org/10.1111/cas.12914 PMID:26918517

16. Bimonte S, Barbieri A, Palma G, Arra C. The role of morphine in animal models of human cancer: does morphine promote or inhibit the tumor growth? Biomed Res Int. 2013; 2013:258141. https://doi.org/10.1155/2013/258141 PMID:24069592

17. Schaal C, Chellappan SP. Nicotine-mediated cell proliferation and tumor progression in smoking-related cancers. Mol Cancer Res. 2014; 12:14–23. https://doi.org/10.1158/1541-7786.MCR-13-0541 PMID:24398389

18. Huhe M, Liu S, Zhang Y, Zhang Z, Chen Z. Expression levels of transcription factors c-Fos and c-Jun and transmembrane protein HAb18G/CD147 in urothelial carcinoma of the bladder. Mol Med Rep. 2017; 15:2991–3000. https://doi.org/10.3892/mmr.2017.6411 PMID:28358415

19. Shan J, Donelan W, Hayner JN, Zhang F, Dudenhausen EE, Kilberg MS. MAPK signaling triggers transcriptional induction of cFOS during amino acid limitation of HepG2 cells. Biochim Biophys Acta. 2015; 1853:539–48. https://doi.org/10.1016/j.bbamcr.2014.12.013 PMID:25523140

20. Shyu PT, Oyong GG, Cabrera EC. Cytotoxicity of probiotics from Philippine commercial dairy products on cancer cells and the effect on expression of cfos and cjun early apoptotic-promoting genes and Interleukin-1 β and Tumor Necrosis Factor-α proinflammatory cytokine genes. Biomed Res Int. 2014; 2014:491740. https://doi.org/10.1155/2014/491740 PMID:25276792

21. Weekes D, Kashima TG, Zandueta C, Perurena N, Thomas DP, Sunters A, Vuillier C, Bozec A, El-Emir E, Miletich I, Patiño-Garcia A, Lecanda F, Grigoriadis AE. Regulation of osteosarcoma cell lung metastasis by the c-Fos/AP-1 target FGFR1. Oncogene. 2016; 35:2852–61. https://doi.org/10.1038/onc.2015.344 PMID:26387545

22. Yamamoto H, Oue N, Sato A, Hasegawa Y, Yamamoto H, Matsubara A, Yasui W, Kikuchi A. Wnt5a signaling is involved in the aggressiveness of prostate cancer and expression of metalloproteinase. Oncogene. 2010; 29:2036–46. https://doi.org/10.1038/onc.2009.496 PMID:20101234

23. Yang Y, Qian Q. Wnt5a/Ca (2+) /calcineurin/nuclear factor of activated T signaling pathway as a potential marker of pediatric melanoma. J Cancer Res Ther. 2014 (10 Suppl); 10:C83–88. https://doi.org/10.4103/0973-1482.145788 PMID:25450290

24. Shojima K, Sato A, Hanaki H, Tsujimoto I, Nakamura M, Hattori K, Sato Y, Dohi K, Hirata M, Yamamoto H, Kikuchi A. Wnt5a promotes cancer cell invasion and proliferation by receptor-mediated endocytosis-dependent and -independent mechanisms, respectively. Sci Rep. 2015; 5:8042. https://doi.org/10.1038/srep08042 PMID:25622531

25. Dorman SN, Viner C, Rogan PK. Splicing mutation analysis reveals previously unrecognized pathways in lymph node-invasive breast cancer. Sci Rep. 2014; 4:7063. https://doi.org/10.1038/srep07063 PMID:25394353

26. Yang AH, Chen JY, Lee CH, Chen JY. Expression of NCAM and OCIAD1 in well-differentiated thyroid carcinoma: correlation with the risk of distant metastasis. J Clin Pathol. 2012; 65:206–12. https://doi.org/10.1136/jclinpath-2011-200416 PMID:22081784

27. Shi Y, Wang J, Xin Z, Duan Z, Wang G, Li F. Transcription factors and microRNA-co-regulated genes in gastric cancer invasion in ex vivo. PLoS One. 2015; 10:e0122882. https://doi.org/10.1371/journal.pone.0122882 PMID:25860484

28. Shukrun R, Pode-Shakked N, Pleniceanu O, Omer D, Vax E, Peer E, Pri-Chen S, Jacob J, Hu Q, Harari-Steinberg O, Huff V, Dekel B. Wilms' tumor blastemal stem cells dedifferentiate to propagate the tumor bulk. Stem Cell Reports. 2014; 3:24–33. https://doi.org/10.1016/j.stemcr.2014.05.013 PMID:25068119

29. Shukrun R, Pode Shakked N, Dekel B. Targeted therapy aimed at cancer stem cells: Wilms' tumor as an example. Pediatr Nephrol. 2014; 29:815–23. https://doi.org/10.1007/s00467-013-2501-0 PMID:23760992

30. Procházková J, Kabátková M, Šmerdová L, Pacherník J, Sykorová D, Kohoutek J, Šimečková P, Hrubá E, Kozubík A, Machala M, Vondráček J. Aryl hydrocarbon receptor negatively regulates expression of the plakoglobin gene (jup). Toxicol Sci. 2013; 134:258–70. https://doi.org/10.1093/toxsci/kft110 PMID:23690540

31. Sheng SH, Zhu HL. Proteomic analysis of pleural effusion from lung adenocarcinoma patients by shotgun strategy. Clin Transl Oncol. 2014; 16:153–57. https://doi.org/10.1007/s12094-013-1054-9 PMID:23907289

32. Aizawa S, Ochiai T, Ara T, Yamada H, Hasegawa H. Heterogeneous and abnormal localization of desmosomal proteins in oral intraepithelial neoplasms. J Oral Sci. 2014; 56:209–14. https://doi.org/10.2334/josnusd.56.209 PMID:25231147

33. Liu P, Jiang W, Zhou S, Gao J, Zhang H. Combined Analysis of ChIP Sequencing and Gene Expression Dataset in Breast Cancer. Pathol Oncol Res. 2017; 23:361–68. https://doi.org/10.1007/s12253-016-0116-z PMID:27654269

34. Nagata M, Noman AA, Suzuki K, Kurita H, Ohnishi M, Ohyama T, Kitamura N, Kobayashi T, Uematsu K, Takahashi K, Kodama N, Kawase T, Hoshina H, et al. ITGA3 and ITGB4 expression biomarkers estimate the risks of locoregional and hematogenous dissemination of oral squamous cell carcinoma. BMC Cancer. 2013; 13:410. https://doi.org/10.1186/1471-2407-13-410 PMID:24006899

35. Nagata M, Kurita H, Uematsu K, Ogawa S, Takahashi K, Hoshina H, Takagi R. Diagnostic value of cyclin-dependent kinase/cyclin-dependent kinase inhibitor expression ratios as biomarkers of locoregional and hematogenous dissemination risks in oral squamous cell carcinoma. Mol Clin Oncol. 2015; 3:1007–13. https://doi.org/10.3892/mco.2015.578 PMID:26623041

36. Wadhwa B, Makhdoomi U, Vishwakarma R, Malik F. Protein kinase B: emerging mechanisms of isoform-

specific regulation of cellular signaling in cancer. Anticancer Drugs. 2017; 28:569–80. https://doi.org/10.1097/CAD.0000000000000496 PMID:28379898

37. Chautard E, Ouédraogo ZG, Biau J, Verrelle P. Role of Akt in human malignant glioma: from oncogenesis to tumor aggressiveness. J Neurooncol. 2014; 117:205–15. https://doi.org/10.1007/s11060-014-1382-9 PMID:24477623

38. Romano G. The role of the dysfunctional akt-related pathway in cancer: establishment and maintenance of a malignant cell phenotype, resistance to therapy, and future strategies for drug development. Scientifica (Cairo). 2013; 2013:317186. https://doi.org/10.1155/2013/317186 PMID:24381788

39. Wilson MI, Dooley HC, Tooze SA. WIPI2b and Atg16L1: setting the stage for autophagosome formation. Biochem Soc Trans. 2014; 42:1327–34. https://doi.org/10.1042/BST20140177 PMID:25233411

40. Hua Y, Ma X, Liu X, Yuan X, Qin H, Zhang X. Identification of the potential biomarkers for the metastasis of rectal adenocarcinoma. APMIS. 2017; 125:93–100. https://doi.org/10.1111/apm.12633 PMID:28028826

41. Cromer MK, Choi M, Nelson-Williams C, Fonseca AL, Kunstman JW, Korah RM, Overton JD, Mane S, Kenney B, Malchoff CD, Stalberg P, Akerström G, Westin G, et al. Neomorphic effects of recurrent somatic mutations in Yin Yang 1 in insulin-producing adenomas. Proc Natl Acad Sci USA. 2015; 112:4062–67. https://doi.org/10.1073/pnas.1503696112 PMID:25787250

42. Munkley J, Lafferty NP, Kalna G, Robson CN, Leung HY, Rajan P, Elliott DJ. Androgen-regulation of the protein tyrosine phosphatase PTPRR activates ERK1/2 signalling in prostate cancer cells. BMC Cancer. 2015; 15:9. https://doi.org/10.1186/s12885-015-1012-8 PMID:25592066

43. Yang LX, Li BL, Liu XH, Yuan Y, Lu CJ, Chen R, Zhao J. RNA-seq reveals determinants of sensitivity to chemotherapy drugs in esophageal carcinoma cells. Int J Clin Exp Pathol. 2014; 7:1524–33. PMID:24817948

44. He RQ, Li XJ, Liang L, Xie Y, Luo DZ, Ma J, Peng ZG, Hu XH, Chen G. The suppressive role of miR-542-5p in NSCLC: the evidence from clinical data and in vivo validation using a chick chorioallantoic membrane model. BMC Cancer. 2017; 17:655. https://doi.org/10.1186/s12885-017-3646-1 PMID:28927388

45. Morris DG, Musat M, Czirják S, Hanzély Z, Lillington DM, Korbonits M, Grossman AB. Differential gene expression in pituitary adenomas by oligonucleotide array analysis. Eur J Endocrinol. 2005; 153:143–51. https://doi.org/10.1530/eje.1.01937 PMID:15994756

46. Michaelis KA, Knox AJ, Xu M, Kiseljak-Vassiliades K, Edwards MG, Geraci M, Kleinschmidt-DeMasters BK, Lillehei KO, Wierman ME. Identification of growth arrest and DNA-damage-inducible gene beta (GADD45beta) as a novel tumor suppressor in pituitary gonadotrope tumors. Endocrinology. 2011; 152:3603–13. https://doi.org/10.1210/en.2011-0109 PMID:21810943

47. Tong Y, Zheng Y, Zhou J, Oyesiku NM, Koeffler HP, Melmed S. Genomic characterization of human and rat prolactinomas. Endocrinology. 2012; 153:3679–91. https://doi.org/10.1210/en.2012-1056 PMID:22635680

48. de Lima DS, Martins CS, Paixao BM, Amaral FC, Colli LM, Saggioro FP, Neder L, Machado HR, dos Santos AR, Pinheiro DG, Moreira AC, Silva WA Jr, Castro M. SAGE analysis highlights the putative role of underexpression of ribosomal proteins in GH-secreting pituitary adenomas. Eur J Endocrinol. 2012; 167:759–68. https://doi.org/10.1530/EJE-12-0760 PMID:22992986

49. Dong X, Liao W, Zhang L, Tu X, Hu J, Chen T, Dai X, Xiong Y, Liang W, Ding C, Liu R, Dai J, Wang O, et al. RSPO2 suppresses colorectal cancer metastasis by counteracting the Wnt5a/Fzd7-driven noncanonical Wnt pathway. Cancer Lett. 2017; 402:153–65. https://doi.org/10.1016/j.canlet.2017.05.024 PMID:28600110

50. Toren P, Kim S, Cordonnier T, Crafter C, Davies BR, Fazli L, Gleave ME, Zoubeidi A. Combination AZD5363 with Enzalutamide Significantly Delays Enzalutamide-resistant Prostate Cancer in Preclinical Models. Eur Urol. 2015; 67:986–90. https://doi.org/10.1016/j.eururo.2014.08.006 PMID:25151012

SUPPLEMENTARY MATERIALS

Supplementary Table

Please browse Full Text version to see the data of Supplementary Table 1.

Supplementary Table 1. Venn diagram of DEGs among four datasets.